

DEVELOPMENT OF AN ONLINE CONTROL SYSTEM FOR A
MULTI-ELEMENT FLUORESCENCE DETECTOR

BURKHARD WRENGER^{b,1}, MARTIN FIEBER-ERDMANN^a, HERMANN
ROSSNER^{b,2} and ELIZABETA HOLUB-KRAPPE^{b,3}

^a*Protein-Struktur-Fabrik, co BESSY GmbH, Albert-Einstein-Str. 15, D-12489 Berlin,
Germany*

^b*Hahn-Meitner-Institut, Berlin, Germany*
E-mail addresses: ²rossner@hmi.de, ³holub – krappe@hmi.de

Paper devoted to honour the memory of Professor Nikola Cindro

Received 25 September 2003; revised manuscript received 30 October 2003
Accepted 8 December 2003 Online 3 March 2004

A new control system for fluorescence and EXAFS studies has been developed consisting of germanium detectors and digital signal processor electronics. Using a standard PC and a new software package leads to a high flexibility regarding application, user interface and use of different synchrotron facilities. The new system achieves spectra with considerably higher quality when compared to a traditional system for fluorescence and EXAFS studies. This allows the investigation of thin films and diluted systems as shown by experiments on a W/Nb multilayer system and on FeS₂ doped with Zn.

PACS numbers: 07.85.Nc, 61.10.Ht

UDC 539.1.074, 539.1.075

Keywords: X-ray absorption, EXAFS, NEXAFS, X-ray spectrometers, fluorescence spectroscopy, Ge detector, digital spectrometer, thin-film multilayers, diluted systems

1. Introduction

Most extended X-ray absorption fine structure (EXAFS) studies have been carried out in the fluorescence mode with sodium iodide (NaI) detectors or in the transmission mode. The energy resolution of NaI-detectors is not sufficient for several sample types whereas the transmission mode usually does not allow the investigation of diluted or thin layer systems. The purpose of the experimental system described here was to overcome the disadvantages mentioned above and to develop a flexible and cost-effective detector system which can easily be used at

¹Present address: FH Lippe und Höxter, An der Wilhelmshöhe 44, D-37671 Höxter

several different synchrotron facilities. Germanium detectors have several advantages when compared to NaI-detectors due to the higher energy resolution. The data acquisition requires pulse amplification and shaping, usually provided by analog electronics. In recent years, the improvement of digital signal processors made higher count rates and lower costs possible when compared to analog systems. As the maximum count rate of the electronics is still a limiting factor, the use of several small detectors is preferred to a single detector of comparable size.

In the present paper, we describe the development of a new type of fluorescence spectrometer consisting of four Ge-detector elements and a digital processor based on Penta-fet electronics. We show the advantages of this spectrometer type when compared to traditional systems for fluorescence and EXAFS studies.

2. *Detector system*

The detector system consists of four high-purity germanium X-ray detectors, each with an active area of 50 mm^2 . Their coaxial geometry results in low capacitance and, therefore, low electronic noise, despite the relatively large active area. The energy range is specified from 200 eV to 200 keV. The detectors are mounted on an element block with an end-cap diameter of 32 mm. Two of them are aligned vertically with closest element spacing and two elements are aligned horizontally in between the former ones.

The detectors are cooled to LN_2 temperature using a 7.5 l dewar and a steel rod that allows the detectors to be transferred up to 203 mm into a vacuum chamber. This movement is achieved by a motor-driven sliding carriage and a welded metal bellow. Electrical isolation is provided between the detector cryostat and vacuum chamber. The temperature of the detectors is measured by a PT100 sensor mounted in the detector-element block. A heat-out resistor in this block is used for the de-icing procedure of the detectors.

The input stage of charge amplifiers used in high-resolution radiation-spectrometers must include two features. The first is a low-noise junction field-effect transistor (FET), and secondly, a charge restoration technique that is efficient and does not degrade the resolution even at high count rate. For this purpose, a specially designed and fabricated five-terminal silicon device [1] is used. This method has some advantages compared to the other restore mechanisms: a) When a pulsed opto-electronic feedback is used for charge restoration, the detector has to be shielded from the effect of light. This is usually achieved by opaque dielectrics which, however, add electronic noise. b) When a high value resistor is connected in the feedback loop, this extra component results in added noise. Using the Penta-fet technique, very low noise performance is achieved. The signals from the FET are amplified to a gain of 3 mV/keV and then fed into the digital spectrometer.

3. *Integration of the detection system*

Software plays an increasing role as an integrating device for different data acquisition systems. The use of software as a inexpensive and flexible replacement for

hardware can often be seen in actual complex experimental setups. This evolution is supported by the development of signal-processor-based detection systems like the one in our experimental setup.

This section starts with a description of the integration of the detectors into our data acquisition system. We discuss the requirements placed on data-acquisition software and the development environment. This section ends with the presentation of the data-acquisition software and a short outlook on improvements of our software system.

3.1. Detection systems and computer hardware

As mentioned earlier, the X-ray detectors are connected using short leads to the XIA digital X-ray processors DXP-4T² which process preamplified signals. In short, every DXP channel consists of four separate units: analog-signal conditioner (ASC), 20 MHz ADC, FiPPI and digital signal processor (DSP). The ASC shapes incoming signals to fit to the ADC. It is monitored and controlled by the DSP. The FiPPI unit (digital filter, peak detector, pileup inspector) performs a preselection of the signals using a fast filter and analyses the signal using a slow filter. Parameters may be tuned using our software (see below). A minimum dead time is achieved by eliminating peaks which follow each other too closely or are too broad, thus giving a maximum count rate of ≈ 300 kHz. The DSP analyses the pulses with respect to their height, controls ASC and FiPPI and is responsible for the communication with the host system. DSP and FiPPI are highly configurable by uploading their software during the initialization period from the host system. The initialization also includes calibration of the preamplifiers. As shown in Fig. 1, the digital X-ray processor DXP 4T is housed in a CAMAC crate, which is controlled via CAMAC interface³ by a standard IBM compatible PC. Also housed in the CAMAC crate are HV power supplies⁴ for detectors and preamplifiers, and a multichannel scaler⁵. The scaler transforms and counts the signals from channeltrons and the incoming beam intensity, which serve, e.g., as reference signals.

Control of the monochromator and of the sample position depends on the experimental environment, i.e. varies with the individual synchrotron radiation facility. In most cases, using our own vacuum chamber, samples are mounted on a motor driven sample manipulator. The motors are controlled by the same LabVIEW software that is described in more details below. Control of the monochromators often makes use of serial or TCP/IP connections and has to be adjusted to each individual monochromator system.

The last step during data acquisition is the backup. As we store every fluorescence spectrum for each Ge detector and for every wavelength of the incident beam, the amount of data is huge compared to standard EXAFS systems. In normal backup mode, a single DXP spectrum with four channels requires ≈ 100 kBytes,

²DXP-4T, X-ray Instrumentation Associates, Newark, CA, www.xia.com.

³CC16, W-IE-NE-R Plein & Baus GmbH, D-Burscheid.

⁴CHQ 221L Dual HV Power supply, ISEG, D-Rosendorf.

⁵Model 84 Quad Scaler, Jorway.

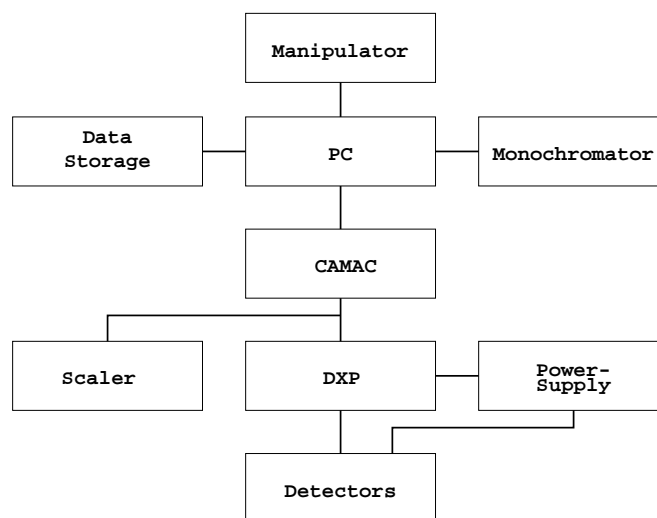


Fig. 1. Data acquisition setup with data and control connections. The whole system is controlled by an IBM-compatible PC, which is connected via CAMAC, serial line or TCP/IP network to monochromator, sample manipulator and DXP (see text). This setup is easily adjusted to the environment found in different synchrotron facilities.

in condensed backup mode about 20% of the normal backup mode. The data file contains underflows, overflows, pile-ups and lifetime in addition to the fluorescence data, thus allowing high quality data analysis. Saving complete fluorescence spectra gives us the possibility to set the region of interest (ROI) during the data analysis process. This is useful, e.g., when energy drifts have to be taken into account.

3.2. Data acquisition software and environment for software development

From the preceding section, we can deduce several requirements for the data-acquisition software and on the software-development system. In particular, it should be easy to adopt to different beam-lines. The software package expects always our four-element Ge detectors and the XIA X-ray processor, but monochromator control varies between individual beam-lines. Common monochromator parameters are start and end energy, size of energy steps ΔE , monochromator speed and type of grid. During a data acquisition run, relevant parameters and results have to be displayed in order to permit an early review of the data. Usually, the software should display the individual fluorescence spectra, region of interest (ROI), electron current, incoming beam intensity and the resulting EXAFS spectrum. Manual tuning of some parameters prior to the data acquisition run allows optimization. In order to support the EXAFS analysis, the size of energy steps ΔE can be switched from $\Delta E = \text{const}$ to $\Delta E \propto \sqrt{E}$. Furthermore, a user-friendly interface and intuitive operation structure should allow short training periods for new users.

We chose LabVIEW as our primary development environment for the following reasons:

- XIA supports individual software by providing low-level software libraries for their DXP products written in Fortran, C or LabVIEW.
- LabVIEW allows short periods of development in technical projects compared to standard development tools.
- LabVIEW separates graphical user interface (“Front Panel”) and data flux (“Connector Panel”) allowing efficient and rapid prototyping of the graphical user interface (GUI).
- Highly-efficient software development leads to a greater number of iteration cycles during a given period of development.
- LabVIEW provides many specialized modules ranging from low-level data-acquisition components to high-level network-services. Modularization of individual programs gives the software developer greater flexibility.
- Code debugging is easy and straightforward.

We use the software modules as a means to provide test components, allowing simulations and fits to individual monochromators. Two disadvantages of LabVIEW should also be mentioned: LabVIEW programs are not very fast in several aspects and support of complex mathematical expressions is poor. As data acquisition and signal shaping is done by the signal processor, the run time performance is sufficient on a 200 MHz Pentium-based PC. The lack of easy coding of complex mathematical expressions is compensated by using off-line data analysis tools.

3.3. *Software system implementation and outlook*

As shown in Fig. 2, the LabVIEW modules – National Instruments calls them virtual instruments (VI) – are grouped in several abstraction layers, the highest level presenting and controlling the user interface. User input is analyzed and sets the parameters in the data acquisition modules. If the whole hardware setup is connected to the system, several low-level VIs have direct access to, e.g., monochromator or digital signal processors. Otherwise, hardware simulation VIs make test runs possible. We developed the simulation VIs in order to run the whole system outside the synchrotron facilities. New software versions and experimental setups can be tested intensively, thus reducing setup-preparation times in the synchrotron facilities to a minimum. For a new version of the XIA DXP software, only the VIs provided by the vendor have to be replaced. Easy upgrading is supported by LabVIEW’s interface system which forces strong type matching.

A window of the GUI is shown in Fig. 3. The small plots at right show electron yield and incoming beam intensity as a reference signal, whereas the central plot is the EXAFS spectrum of the Ge-detectors in a given ROI. The lower part of the window contains informations about, e.g. the progress of the spectrum, actual monochromator energy and energy steps or type and file name of the data backup.

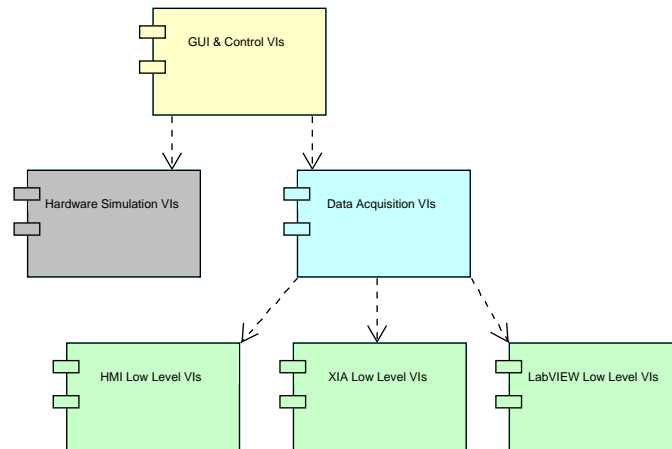


Fig. 2. The Unified Modelling Language (UML) component diagram shows the relations within the LabVIEW VIs used in our software package. The separation of user-interface components and data-acquisition components allows us to run extensive prior tests off beamline (e.g. outside any synchrotron facility). This is done by replacing the data acquisition VIs by hardware simulation VIs. The second component separation leads to a XIA low-level package, which helps to reduce our efforts when a new version of the XIA software has to be integrated.

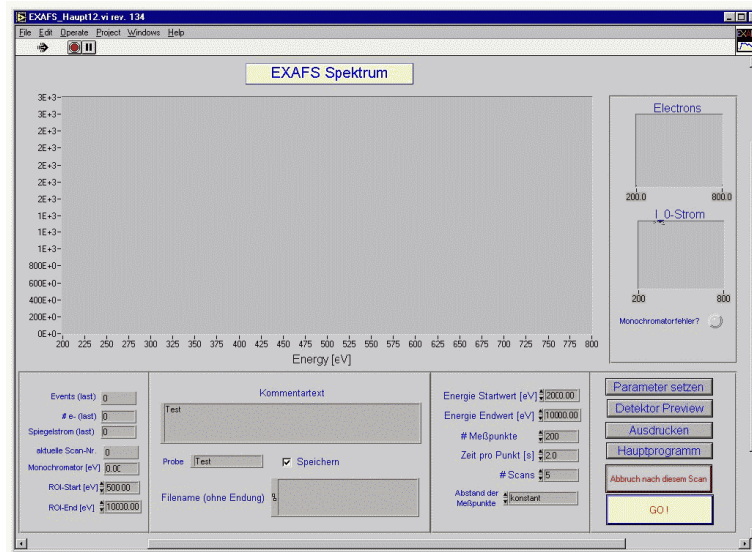


Fig. 3. User interface for our data acquisition software at the beginning of the run. The essential informations during a data acquisition run are the EXAFS spectrum, electron beam and incoming beam intensity as reference signals, ROI and monochromator settings. Individual fluorescence spectra, events or the lifetime of individual channels can be displayed in a different window, not shown here.

The individual fluorescence spectra are displayed in another window not shown here. The online observation of fluorescence spectra and reference signals allows an effective recognition of problems and an optimization of the yield. Usually, this is done by changing, e.g. signal-shaping parameters in the digital signal processor.

As the XIA DXP allows a time resolution down to $50 \mu\text{s}$, time-resolved EXAFS spectra seem to be possible if the flux of the incident beam is of sufficient intensity.

3.4. Application and results

In this section, we show two examples for the application of a digital X-ray spectrometer combined with a four-element Ge detector for NEXAFS (near edge X-ray absorption fine structure) and EXAFS spectra and compare it with the results from a standard NaI-spectrometer. All experimental data have been obtained at the HASYLAB synchrotron facility in Hamburg.

In the first example, we apply the two types of detectors in the case of a very diluted system. We took NEXAFS spectra at the Zn K-edge in pyrite (FeS_2) doped with 3% of Zn. The crystal was grown at the Hahn-Meitner-Institute Berlin in the group of S. Fiechter and was of interest for applications in solar energy studies. Experiments have been performed at the E4 beamline at HASYLAB. Figure 4a

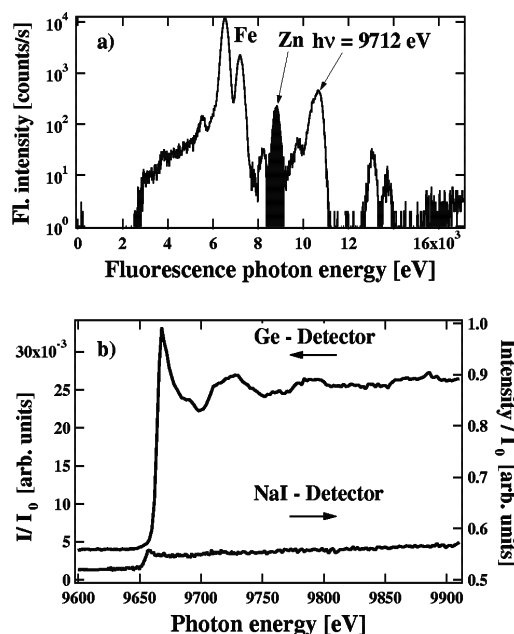


Fig. 4. Fluorescence spectrum taken by a single Ge-detector at a photon energy of 9712 eV for FeS_2 doped with 3% Zn. The shaded area denotes the Zn K_α region over which we will integrate for further data analysis. b) NEXAFS spectrum at the Zn K-edge (9659 eV) obtained by the four-element Ge-detector (upper curve) and by using the NaI-detector (lower curve).

shows a fluorescence spectrum obtained at a photon energy of 9712 eV, measured with one single Ge-detector in the four-element Ge-detector system.

The X-ray emission (fluorescence) lines of Fe K_{α} (at 6400 eV), Fe K_{β} (at 7060 eV), Zn K_{α} (shaded area, peak at about 8630 eV) and the elastic scattering line ($h\nu = 9712$ eV) are clearly resolved. The strong sulphur K_{α} peak (at 2307 eV) has been cut off by the threshold of the detector to reduce the count rate. With the energy resolution achieved, a much smaller ROI for the peak of interest is possible, as compared to a standard NaI-detector system, allowing element-specific data acquisition. This reduces the dead time of the data-acquisition electronics, allowing higher effective count rates. In fact, effective count rates of more than 250 000 counts per second are possible for every channel. Using a NaI-detector system, it would not be possible to focus on the Zn K_{α} peak as the peaks of Fe and elastic scattering peak have significantly higher intensities and the energy resolution of the detector does not allow to resolve them. The complete NEXAFS spectra are obtained by taking the fluorescence spectra as shown in Fig. 4a for each of four Ge-detectors and scanning the excitation photon energy through the NEXAFS energy range of the Zn K-edge ($h\nu = 9600 - 9910$ eV). In Figs. 4a and b, the NEXAFS curve related to the data gained by using the Ge-detector is obtained by integrating over the Zn K_{α} peak (the shaded area in Fig. 4a) for each of the four Ge-detectors and at each measured photon energy. For comparison, we show the same spectra obtained by using the standard NaI detector. The gain of useful information from absorption spectra, employing the digital X-ray spectrometer and the multielement Ge-detector system, compared to the application of the NaI detector system is obvious. While the NaI detector gives only a slight indication of the absorption edge of the element of interest for diluted systems, with the multielement Ge-detectors we are obtaining results which can be used for typical absorption-data analysis (NEXAFS and EXAFS).

Another example for the use of the four-element Ge-detector system, compared to the NaI-detector system, is a sample consisting of a W and Nb multilayer system, a sequence of [2.6 nm W/10 nm Nb]*60 grown on a MgO(001) crystal. This system was exposed at a temperature of 185 °C in a hydrogen atmosphere of varying pressure ($p(\text{H}_2) = 10^{-4}$ to 1000 mbar). Hydrogen was absorbed only in the Nb film, causing structural changes in the macroscopic thickness of the Nb film and microscopic structural changes in the Nb interatomic distances. The Nb film had a bcc structure and was grown in (001) orientation. Upon hydrogen intercalation, the first-neighbour distances of a bcc Nb crystal, R_1 (distance of body centred atom to the corner atom) and R_2 (distance of the first neighbouring corner atoms) are both increased due to hydrogen intercalation. This structural change is hydrogen-pressure dependent. Neutron scattering and synchrotron EXAFS experiments have been performed to study these structural changes (see a more detailed description in Refs. [2], [3] and [4]). EXAFS experiments were performed at the X1.1 experimental station at HASYLAB and only they could give the essential information to understand the structural changes giving both, the in-plane and out-of-plane structural changes of the Nb film upon hydrogen intercalation. For this system, we could use both, the NaI and the multielement Ge-detector data, but as we will show

in the following, the quality of the Ge data was much better. EXAFS experiments have been performed at the Nb K-edge at 18985 eV.

In Fig. 5, we present one example of EXAFS data for the above system obtained with the NaI-detector and the corresponding EXAFS data analysis. These data are more extensively described in Refs. [2] and [4]. In part (a) of the figure, we show the EXAFS spectrum at the Nb K-edge, taken at normal incidence of the light on the film surface. The data are shown for a hydrogen pressure of 1 mbar. In part (b) is shown the corresponding EXAFS $\chi(k)$ function and the fit of the data, using the FEFF code [5], and in part (c), the Fourier transformation of these data into R -space giving interatomic distances R_1 and R_2 in the most pronounced peak. The corresponding two peaks are part of the main peak and could be resolved into both components by the deconvolution of the spectrum using again the FEFF code.

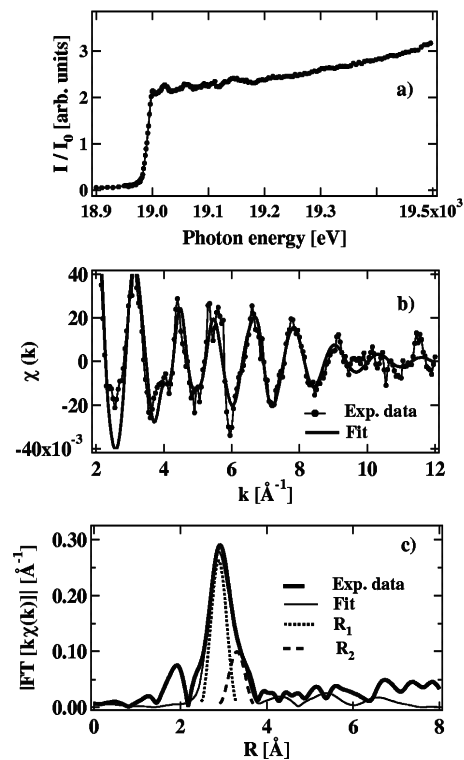


Fig. 5. a) EXAFS spectrum taken at the Nb K-edge (18895 eV) with normal incidence of the light on the sample surface for the $[2.6 \text{ nm W}/10 \text{ nm Nb}] \times 60$ multilayer system, using a NaI-detector. b) The experimental EXAFS $\chi(k)$ function obtained from a) and the fit to the data using the FEFF code [5]. c) The corresponding Fourier transformation FT of the data presented in b) in R -space (the radial distribution function on Nb atomic distances) together with the fit by the FEFF code and the deconvolution in the first two nearest-neighbour-distance components R_1 and R_2 .

In Figs. 6 and 7, we show the same kind of data as in the former figure (normal incidence, taken at a hydrogen pressure of 1 mbar) obtained this time with the four-element Ge-detector and the digital X-ray spectrometer. In Fig. 6, we present the

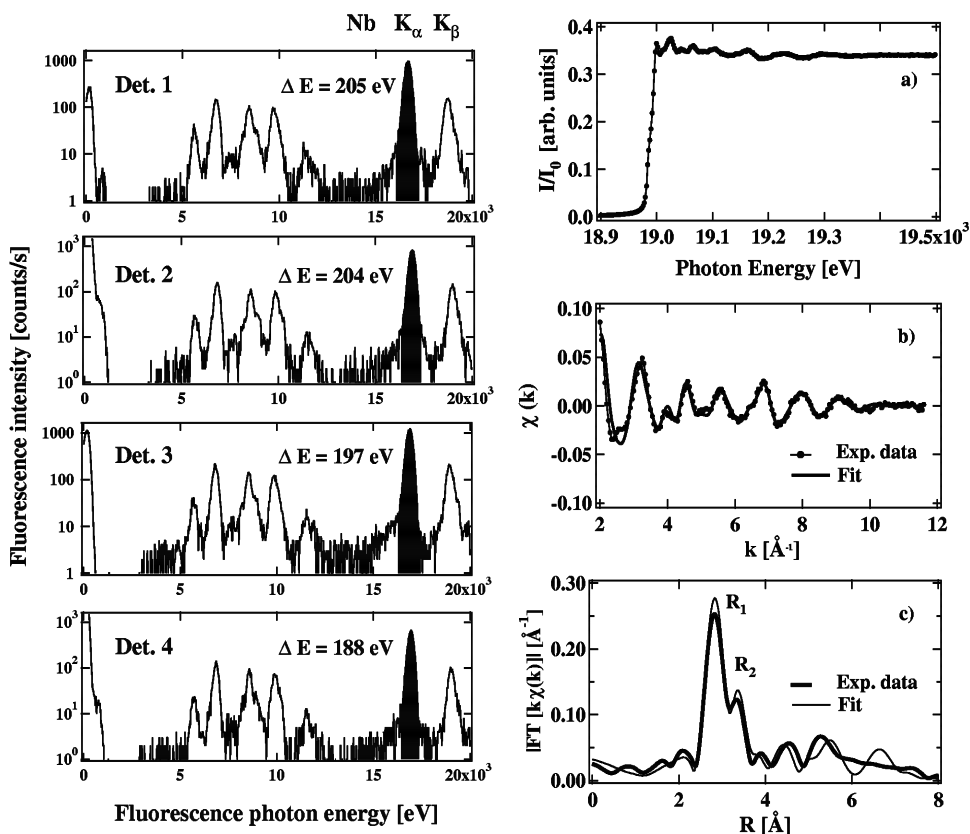


Fig. 6 (left). Fluorescence spectra for the $[2.6 \text{ nm W}/10 \text{ nm Nb}]^*60$ multilayer system taken at a photon energy of 19500 eV in normal incidence, using the four-element Ge-detector system and the digital X-ray spectrometer. The energy resolution of each Ge-detector and the Nb $K\alpha$ (the shaded area) and $K\beta$ peaks are explicitly shown.

Fig. 7 (right). a) EXAFS spectrum for the Nb K-edge (18985.6 eV) of the $[2.6 \text{ nm W}/10 \text{ nm Nb}]^*60$ multilayer system, taken at normal incidence of the light on the sample under 1 mbar hydrogen pressure, using the integral over the Nb $K\alpha$ line (the shaded area in Fig. 6) of each Ge-detector at each incident photon energy. b) The experimental EXAFS $\chi(k)$ function obtained from a) and the fit to the data using the FEFF code [5]. c) The Fourier transformation FT of the data b) into R-space (the radial distribution function) for Nb interatomic distances, together with the fit by the FEFF code. The first two nearest-neighbour-distance components R_1 and R_2 are well separated.

typical fluorescence spectra for each of the four Ge-detectors for the same W/Nb multilayer system. The last two strong peaks in the fluorescence spectra correspond to Nb K_α and K_β peaks. The shaded area represents the Nb K_α peak (with the corresponding energy resolution of the detector) over which the integration was performed at each photon energy to obtain the resulting EXAFS spectrum shown in Fig. 7a. Fig. 7b presents the EXAFS $\chi(k)$ function and the fit of the data using the FEFF code. Comparing only the EXAFS functions obtained by NaI- and Ge-detectors, we observe much stronger EXAFS oscillations and stronger intensities in the $\chi(k)$ function, due to the element sensitivity and the higher count rate of the Ge-detector. Fourier transformation to R -space, shown in Fig. 7c, gives, this time, well resolved R_1 and R_2 components. The changes of the R_2 distance upon hydrogen intercalation with increasing hydrogen pressure were essential to understand the macroscopic film-thickness changes and microscopic interatomic distances of the Nb film. EXAFS data offered this structural information [3].

3.5. Summary

The use of a Ge-detector system combined with charge amplification by the Penta-fet technique is characterised by low noise and high resolution. The digital-signal-processor electronics for pulse shaping and analysis allows count rates up to 300 kHz. Our central data processing unit consists of a standard IBM compatible PC with a CAMAC interface to the digital signal processor system. The LabVIEW software package developed by the Hahn-Meitner-Institute controls the data acquisition and the experimental setup, like sample manipulator or beamline monochromator. It has proven to be a flexible, reliable and inexpensive replacement for a standard hardware pulse-shaping and data-acquisition system for fluorescence experiments. From the two examples shown to demonstrate the use of the digital X-ray spectrometer in combination with the multielement Ge-fluorescence detector system, it is clear that for diluted systems, the use of the Ge-detectors is of essential importance in order to obtain structural information from absorption-spectroscopy methods. This use becomes increasingly important for the study of the local structure of biological systems and for environmental studies. But even in cases where the use of NaI-detectors as fluorescence detector is in principle possible, the quality of the data is considerably increased by using the X-ray digital spectrometer and the multielement Ge-detector system. The advantage of the X-ray digital spectrometer and the peak integration/analysis procedures, performed after the data acquisition, are clearly seen and particularly important in cases where the fluorescence peaks of the various elements of the system are close to the fluorescence peak of the EXAFS emitter. This is especially important in the case of low concentration of these elements. For NEXAFS and EXAFS studies of elements with very low concentration, the use of Ge-detectors with high number of elements is necessary. The presented data-acquisition and analysis method can be extended for the application on such multielement-detector systems.

References

- [1] T. Nashashibi and G. White, IEEE Transactions on Nuclear Science **37** (1990) 452.
- [2] Ch. Rehm, *Wasserstoff in dünnen metallischen Systemen*, PhD Thesis, Technische Universität, Berlin (1999).
- [3] H. Maletta, Ch. Rehm, F. Klose, M. Fieber-Erdmann and E. Holub-Krappe, J. Magn. and Magn. Materials **240** (2002) 475.
- [4] F. Klose, Ch. Rehm, M. Fieber-Erdmann, E. Holub-Krappe, H. J. Bleif, H. Sowers, R. Goyette, L. Tröger and H. Maletta, Physica B **283** (2000) 184.
- [5] S. I. Zabinsky, J. J. Rehr, A. Ankudinov, R. C. Albers and M. J. Eller, Phys. Rev. B **52** (1995) 2995.

RAZVOJ RAČUNALNOG UPRAVLJAČKOG SUSTAVA ZA VIŠEDJELNI
FLUORESCENTNI DETEKTOR

Razvili smo upravljački sustav za proučavanje fluorescencije i EXAFS koji se sastoji od germanijskih detektora i signalne digitalne procesorske elektronike. Primjenom standardnog osobnog računala i novog programskog paketa, postigli smo veliku prilagodljivost u primjenama, s međujedinicama i za različite sinkrotronske postave. Nov sustav postiže znatno bolje spektre u usporedbi s uobičajenim sustavima za proučavanje fluorescencije i EXAFS. Tako su moguća istraživanja tankih slojeva i razrijeđenih otopina, kako pokazujemo s višeslojnim W/Nb i sa Zn-punjenim FeS₂.